

JPET#249904

**The antinociceptive and anti-inflammatory properties of the  $\alpha 7$  nAChR weak partial agonist  $p$ -  
 $CF_3$   $N,N$ -diethyl- $N'$ -phenylpiperazine**

Marta Quadri, Deniz Bagdas, Wisam Toma, Clare Stokes, Nicole A. Horenstein, M. Imad Damaj, Roger. L.  
Papke

*Department of Pharmacology and Therapeutics, University of Florida, PO Box 100267, Gainesville, FL 32610-0267, USA  
(M.Q., C.S., R.L.P.)*

*Department of Chemistry, University of Florida, PO Box 117200, Gainesville, FL 32611-7200, USA (M.Q., N.A.H.)*

*Department of Pharmacology and Toxicology, Medical College of Virginia, Virginia Commonwealth University, Richmond,  
VA 23298-0613, USA (D.B., W.T., M.I.D.)*

JPET#249904

**Running Title: Antinociceptive and anti-inflammatory nAChR weak partial agonist**

Address correspondence to: Roger L. Papke, Department of Pharmacology and Therapeutics, University of Florida, P.O. Box 100267, Gainesville, FL 32610-0267. Phone number: 352-392-4712. Fax number: 352-392-3558. E-mail: rlpapke@ufl.edu

Number of text pages:	17
Number of tables:	0
Number of figures:	11
Number of references:	48
Number of words in the Abstract:	244
Number of words in the Introduction:	784
Number of words in the Discussion:	1302

**Abbreviations:**

BL, baseline; CFA, complete Freund's adjuvant; CRC, concentration-response curve; D<sub>i</sub>, PAM-insensitive nonconducting desensitized state; diEPP, *N,N*-diethyl-*N'*-phenylpiperazinium iodide; D<sub>s</sub>, PAM-sensitive nonconducting desensitized state; ΔPD, difference in the ipsilateral paw diameter; F<sub>dose</sub>, bioavailability dose; i.p., intraperitoneal; i.pl., intraplantar; LPS, lipopolysaccharide; MLA, methyllycaconitine; nAChR, nicotinic

JPET#249904

acetylcholine receptor; *p*-CF<sub>3</sub>, para-trifluoromethyl; PAM, positive allosteric modulator; RIC3, resistance-to-cholinesterase 3; s.c., subcutaneous; TNF, tumor necrosis factor; TQS, 4-naphthalene-1-yl-3a,4,5,9b-tetrahydro-3-*H*-cyclopenta[*c*]quinoline-8-sulfonic acid amide; Veh, vehicle; Veh/Veh, vehicle-vehicle.

JPET#249904

## ABSTRACT

Chronic pain and inflammatory diseases can be regulated by complex mechanisms involving  $\alpha 7$  nicotinic acetylcholine receptors (nAChRs), making this subtype a promising drug target for anti-inflammatory therapies. Recent evidence suggests that such treatment of inflammatory pain may rely on metabotropic-like rather than ionotropic activation of the  $\alpha 7$  receptor subtype in non-neuronal cells. We previously identified *p*-CF<sub>3</sub> *N,N*-diethyl-*N'*-phenylpiperazinium (diEPP) iodide to be among the compounds classified as silent agonists, which are very weak  $\alpha 7$  partial agonists that are able to induce positive allosteric modulator (PAM)-sensitive desensitization. Such drugs have been shown to selectively promote  $\alpha 7$  ionotropic-independent functions. Therefore, we here further investigated the electrophysiological profile of *p*-CF<sub>3</sub> diEPP and its *in vivo* antinociceptive activity using *Xenopus* oocytes expressing  $\alpha 7$ ,  $\alpha 4\beta 2$ , or  $\alpha 3\beta 4$  nAChRs. The evoked currents confirmed *p*-CF<sub>3</sub> diEPP to be  $\alpha 7$ -selective with a maximal agonism 5% that of ACh. Co-application of *p*-CF<sub>3</sub> diEPP with the type II PAM TQS produced desensitization that could be converted to PAM-potentiated currents, which at a negative holding potential were up to 13-fold greater than ACh controls. Voltage-dependence experiments indicated that channel block may limit both control ACh and TQS-potentiated responses. Although no *p*-CF<sub>3</sub> diEPP agonist activity was detected for the heteromeric nAChRs, it was a noncompetitive antagonist of these receptors. The compound displayed remarkable anti-hyperalgesic and anti-edema effects in *in vivo* assays. The antinociceptive activity was dose- and time-dependent. The anti-inflammatory components were sensitive to the  $\alpha 7$ -selective antagonist methyllycaconitine, which supports the idea that these effects are mediated by the  $\alpha 7$  nAChR.

JPET#249904

## 1. INTRODUCTION

Although the basis for nicotinic acetylcholine receptor (nAChR) signaling has been associated with ion channel activity and receptor permeability to cations ( $\text{Na}^+$ ,  $\text{K}^+$ , and  $\text{Ca}^{2+}$ ) upon binding of specific ligands, the  $\alpha 7$  nAChR subtype also displays an additional pharmacology related to a mode of signal transduction (Horenstein and Papke, 2017). Besides being widely distributed in the central and peripheral nervous systems, especially in the brain, the  $\alpha 7$  nAChR has been found in non-neuronal cells and tissues not associated with ion channel transmission, such as lymphocytes, macrophages, and microglial cells (Fujii et al., 2017; Zdanowski et al., 2015). These non-neuronal cells are involved in the modulation of immune responses and neuropathic pain through the anti-inflammatory cholinergic pathway, which involves communication between the nervous and immune systems mediated by the vagal nerve (Tracey, 2007). Although the mechanisms regulating cytokine production and release are complex, the involvement of  $\alpha 7$  nAChR has been extensively demonstrated (Horenstein and Papke, 2017; Tracey, 2007; Papke et al., 2015). In immune cells, the  $\alpha 7$  nAChR appears to function as a metabotropic-like receptor (Papke, 2014a; Kabbani and Nichols, 2018) by interacting with different pathways (i.e. JAK/STAT) (de Jonge et al., 2005), regulating tumor necrosis factor (TNF) release from macrophages (Thomsen and Mikkelsen, 2012), and potentially coupling with G-proteins (Kabbani et al., 2013; King et al., 2015). Therefore, the  $\alpha 7$  receptor subtype emerged as a promising target to treat disorders including inflammatory diseases and chronic neuropathic pain (Papke et al., 2015).

Modulation of the  $\alpha 7$  non-ionotropic effects may represent a better and alternative approach to classic ionotropic receptor activation to control and induce anti-inflammatory responses. Because of the diversity found in the distribution and functions of  $\alpha 7$  nAChRs in the human body, molecules selectively promoting  $\alpha 7$  non-ionotropic signaling may reduce off-target effects compared to compounds inducing current-dependent effects, and therefore promote anti-inflammatory responses over cognitive effects. Some of the molecules selectively able to promote the  $\alpha 7$  metabotropic-like function are known as silent agonists (Quadri et al., 2017a; Quadri et al., 2017b; Quadri et al., 2016; Chojnacka et al., 2013; Papke et al., 2014b). Silent agonists are very weak  $\alpha 7$

JPET#249904

partial agonists with the capability of selectively inducing and stabilizing receptor desensitization, which can be revealed by co-application of a type II positive allosteric modulator (PAM) such as PNU-120596 (*N*-(5-chloro-2,4-dimethoxyphenyl)-*N'*-(5-methyl-3-isoxazolyl)-urea) (Grønlien et al., 2007; Hurst et al., 2005) or TQS (4-naphthalene-1-yl-3a,4,5,9b-tetrahydro-3-*H*-cyclopenta[*c*]quinoline-8-sulfonic acid amide) (Grønlien et al., 2007) (**Figure 1**).  $\alpha 7$  type II PAMs bind to sites distinct from the orthosteric agonist sites and do not induce significant receptor activation on their own but rather act on receptor agonist activation and/or desensitization by increasing  $\alpha 7$ 's intrinsically low open probability ( $P_{\text{open}}$ ) by means of at least two mechanisms. PAMs may reduce the steep energy barrier to enter the open state(s) and/or may decrease  $\alpha 7$  desensitization by destabilizing the receptor's desensitized state and inducing a PAM-sensitive, kinetically coupled conductive state. The combination of those two components results in activation of desensitized receptors, (Williams et al., 2011a), allowing type II PAMs to reveal  $\alpha 7$  desensitization induced by silent agonists. The  $\alpha 7$ -selective silent agonist NS6740 (1,4-diazabicyclo[3.2.2]nonan-4-yl(5-(3-(trifluoromethyl)phenyl)furan-2-yl)methanone) (**Figure 1**), which induces strong desensitization but very little ion channel activation, proved to be efficacious in *in vitro* and *in vivo* inflammatory models (Papke et al., 2015; Thomsen and Mikkelsen, 2012). Indeed, in microglia cells NS6740 was more effective in reducing LPS (lipopolysaccharide)-induced TNF- $\alpha$  release compared to efficacious  $\alpha 7$  agonists such as choline (Thomsen and Mikkelsen, 2012). Moreover, different mouse models of chronic pain were investigated for testing the anti-inflammatory activity of NS6740, and the drug was efficacious for reducing inflammation associated with tonic inflammatory pain and peripheral neuropathy. In these models, the effects of NS6740 were consistent with non-ionotropic signaling transduction (Papke et al., 2015).

Here we report our investigation of the anti-inflammatory profile of a weak  $\alpha 7$  partial agonist with a low channel activation efficacy, comparable to that of NS6740 but with a different molecular framework and more readily reversible desensitization. Structural modifications of the weak  $\alpha 7$  silent agonist diEPP (*N,N*-diethyl-*N'*-phenylpiperazinium) (Papke et al., 2014b) (**Figure 1**) led to the identification of a much deeper desensitizer, related to a trifluoromethyl group in the para position of the aromatic ring, 1,1-diethyl-4-(4-

JPET#249904

(trifluoromethyl)phenyl)piperazin-1-ium iodide (*p*-CF<sub>3</sub> diEPP) (Quadri et al., 2016) (**Figure 1**). Indeed, by introducing the *p*-CF<sub>3</sub> group, we achieved a substantial increase in the PNU-120596-potentiated response compared to the parent compound diEPP while preserving the very weak partial agonist component. To better define the pharmacological profile of this promising  $\alpha 7$  very weak partial agonist, we expanded the investigation of its effects on different nAChR subtypes and with the alternative type II PAM, TQS. Together with these extensive electrophysiological characterizations, we report the highlights of *p*-CF<sub>3</sub> diEPP effects in *in vivo* models of hyperalgesia and edema.

## 2. MATERIALS AND METHODS

### 2.1. *In vitro* methods

#### 2.1.1. *Heterologous expression of nAChRs in Xenopus laevis oocytes*

*Xenopus laevis* oocytes were injected with human nAChR clones obtained from Dr. J. Lindstrom (University of Pennsylvania, Philadelphia, PA) to heterologously express nAChRs. To improve the level and speed of  $\alpha 7$  subtype expression without affecting its pharmacological properties (Halevi et al., 2003), the human resistance-to-cholinesterase 3 (RIC3) clone was coinjected with  $\alpha 7$ . RIC3 was obtained from Dr. M. Treinin (Hebrew University, Jerusalem, Israel). Plasmid cDNAs were first linearized and purified, then cRNAs were prepared using the mMessage mMachin *in vitro* RNA transcription kit (Ambion, Austin, TX). Oocytes were surgically removed from mature *Xenopus laevis* frogs (Nasco, Ft. Atkinson, WI) and subsequently injected with appropriate nAChR subunit cRNAs as described previously (Papke and Stokes, 2010). Frogs were maintained in the Animal Care Service facility of the University of Florida, and all procedures were approved by the University of Florida Institutional Animal Care and Use Committee. All studies were carried out in accordance with the National Institutes of Health's Guide for the Care and Use of Laboratory Animals. Briefly, the frog was first anesthetized for 15-20 min in 1.5 L frog tank water containing 1 g of 3-aminobenzoate methanesulfonate buffered with sodium bicarbonate. The harvested oocytes were treated with 1.25 mg/ml collagenase

JPET#249904

(Worthington Biochemicals, Freehold, NJ) for 2 h at room temperature in a calcium-free Barth's solution (88 mM NaCl, 1 mM KCl, 2.38 mM NaHCO<sub>3</sub>, 0.82 mM MgSO<sub>4</sub>, 15 mM HEPES, and 12 mg/l tetracycline, pH 7.6) to remove the follicular layer. Stage V oocytes were subsequently isolated and injected with 50 nl of 5-20 ng nAChR subunit cRNA. Recordings were carried out 1-7 days after injection.

### 2.1.2. Chemicals

Solvents and reagents were purchased from Sigma. Cell culture supplies were purchased from Invitrogen. *p*-CF<sub>3</sub> diEPP (1,1-diethyl-4-(4-(trifluoromethyl)phenyl)piperazin-1-ium iodide) was synthesized as described previously (Quadri et al., 2016). TQS (4-naphthalene-1-yl-3a,4,5,9b-tetrahydro-3-*H*-cyclopenta[*c*]quinoline-8-sulfonic acid amide) was synthesized as described previously by Dr. Ganesh A. Thakur (Kulkarni and Thakur, 2013). Fresh acetylcholine (ACh) stock solutions were made each day of experimentation. TQS and *p*-CF<sub>3</sub> diEPP stock solutions were prepared in DMSO, stored at -20 °C, and used for up to 1 month. TQS and *p*-CF<sub>3</sub> diEPP solutions were prepared fresh each day at the desired concentration from the stored stock.

### 2.1.3 Two-electrode voltage clamp electrophysiology

Experiments were conducted using OpusXpress 6000A (Molecular Devices, Union City, CA). The OpusXpress recording system has previously been described in detail (Papke and Stokes, 2010). In brief, OpusXpress provides two-electrode voltage clamp of 8 oocytes in parallel, including steady bath perfusion, drug delivery, and data acquisition. Both the voltage and current electrodes were filled with 3 M KCl. Oocytes were voltage-clamped at -60 mV unless otherwise specified. For voltage-dependent experiments, oocytes were also voltage-clamped at -90 mV, -70 mV, -50 mV, and -30 mV throughout the whole experiment, including delivery of ACh controls, when *p*-CF<sub>3</sub> diEPP was co-applied with ACh or also at +50 mV immediately prior to and during testing compound *p*-CF<sub>3</sub> diEPP co-applied with TQS. The oocytes were bath-perfused with Ringer's solution (115 mM NaCl, 2.5 mM KCl, 1.8 mM CaCl<sub>2</sub>, 10 mM HEPES, and 1 mM atropine, pH 7.2) at 2 ml/min



JPET#249904

for  $\alpha 7$  receptors and at 4 ml/min for other subtypes. To evaluate the effects of experimental compounds compared to ACh-evoked responses of various nAChR subtypes expressed in oocytes, baseline control ACh responses were defined by two initial applications of ACh made before co-applications of experimental compounds with the control ACh. The agonist solutions were applied from a 96-well plate via disposable tips, and the test compounds were applied alone, co-applied with ACh, or co-applied with TQS. For the concentration-response study, drug applications alternated between ACh controls and experimental compounds to insure the stability of the baseline responses. Unless otherwise indicated, drug applications were 12 s in duration followed by a 181 s washout period for  $\alpha 7$  receptors and 6 s with a 241 s washout for other subtypes. A typical recording for each oocyte constituted two initial control applications of ACh, an experimental compound application, and then a follow-up control application of ACh to determine the desensitization or possible rundown of the receptors. The control ACh concentrations were 60  $\mu$ M for  $\alpha 7$ , 30  $\mu$ M for  $\alpha 4\beta 2$ , and 100  $\mu$ M for  $\alpha 3\beta 4$ . The responses of  $\alpha 4\beta 2$  and  $\alpha 3\beta 4$ -expressing cells were measured as peak current amplitudes, and the  $\alpha 7$  data were calculated as net charge, as previously described (Papke and Porter Papke, 2002). Data were collected at 50 Hz, filtered at 20 Hz, analyzed by Clampfit 9.2 (Molecular Devices) and Excel 2003 (Microsoft, Redmond, WA), and normalized to the averaged peak current or net-charge response of the two initial ACh controls (Papke and Porter Papke, 2002). Data were expressed as means  $\pm$  S.E.M. from at least four oocytes for each experiment and plotted by KaleidaGraph 4.1.1 (Abelbeck Software, Reading, PA). Receptor-mediated activity has a limit of detection of approximately 0.05% of the ACh controls.

Multi-cell averages were calculated for display and comparisons of the raw data. Data from each cell were baseline-corrected by subtracting the mean of the holding current for a 30 s period prior to the control ACh solution. The data were then normalized by dividing the control and experimental data by the peak current of the control response for each cell. Averages of the normalized data were calculated for each of the 10,322 points in each of the 206.44 s traces (acquired at 50 Hz), as well as the standard errors for those averages.\

## 2.2. *In vivo methods*

JPET#249904

### 2.2.1. *Animals*

Male adult (8-10 weeks of age) ICR mice obtained from Harlan Laboratories (Indianapolis, IN). Mice were housed in a 21°C humidity-controlled Association for Assessment and Accreditation of Laboratory Animal Care–approved animal care facility. They were housed in groups of four and had free access to food and water. The rooms were on a 12-hour light/dark cycle (lights on at 7:00 AM). All experiments were performed during the light cycle (between 7:00 AM and 7:00 PM), and the study was approved by the Institutional Animal Care and Use Committee of Virginia Commonwealth University. All studies were carried out in accordance with the National Institutes of Health’s Guide for the Care and Use of Laboratory Animals. Animals were sacrificed via CO<sub>2</sub> following by cervical dislocation after the experiments finished, unless noted otherwise. Any subjects that subsequently showed behavioral disturbances unrelated to the pain induction procedure were excluded from further behavioral testing.

### 2.2.2. *Drugs*

Methyllycaconitine citrate (MLA) was purchased from RBI (Natick, MA). Complete Freund’s adjuvant (CFA) was purchased from Sigma-Aldrich (St. Louis, MO). *p*-CF<sub>3</sub> diEPP (1,1-diethyl-4-(4-(trifluoromethyl)phenyl)piperazin-1-ium iodide) was synthesized as previously described (Quadri et al., 2016) and was dissolved in a mixture of 2:2:16 [2 volume ethanol/2 volume Emulphor-620 (Rhone-Poulenc, Inc., Princeton, NJ)/16 volumes distilled water] and administered intraperitoneally (i.p.) for systemic injections. MLA was dissolved in physiologic saline (0.9% sodium chloride) and injected subcutaneously (s.c.) at a total volume of 1 ml/100 g body weight, unless noted otherwise. All doses are expressed as the free base of the drug.

### 2.2.3. *Complete Freund’s adjuvant (CFA)-induced inflammatory pain model*

We explored the effects of *p*-CF<sub>3</sub> diEPP in the CFA test, composed of inactivated and dried *Mycobacterium tuberculosis* and adjuvant, a widely used model of persistent inflammatory pain. The CFA

JPET#249904

model is based on hypersensitivity, paw swelling, and nuclear factor- $\kappa$ B (NF- $\kappa$ B) mediated transcription of tumor necrosis factor- $\alpha$  (TNF $\alpha$ ) involved in the formation of the principal mediators of inflammation (Hartung et al., 2015). Mice were injected intraplantarly (i.pl.) with 20  $\mu$ L of CFA (50%, diluted in mineral oil). Mechanical sensitivity (see measurement of von Frey test) and paw diameter were measured before and 3 days after CFA injection. *p*-CF<sub>3</sub> diEPP (1, 3.3, and 10 mg/kg) or vehicle were injected intraperitoneally (i.p.) on day 3 after CFA injection, and mice were tested for mechanical sensitivity at different time points (15, 30, 60 and 120 min) after drug injection.

We determined the  $\alpha$ 7 nAChRs mediation in the effects of *p*-CF<sub>3</sub> diEPP using s.c. injection of the  $\alpha$ 7 antagonist MLA in a separate group of mice.  $\alpha$ 7 nicotinic antagonist MLA (10 mg/kg) or vehicle (saline) was injected subcutaneously (s.c.) 15 min before the *p*-CF<sub>3</sub> diEPP (10 mg/kg; i.p.) or vehicle injection. Mechanical sensitivity was then tested 30 min after and paw diameter was measured 1 h after *p*-CF<sub>3</sub> diEPP injection.

#### 2.2.4. Evaluation of mechanical sensitivity

Mechanical sensitivity thresholds were determined according to the method of Chaplan et al. (Chaplan et al., 1994) and as adapted in Bagdas et al. (Bagdas et al., 2015). A series of calibrated von Frey filaments (Stoelting, Wood Dale, IL) with logarithmically incremental stiffness ranging from 2.83 to 5.07 expressed as dsLog 10 of [10 x force in (mg)] were applied to the paw with a modified up-down method (Dixon, 1965). The mechanical threshold was expressed as Log10 of [10 x force in (mg)], indicating the force of the Von Frey hair to which the animal reacted (paw withdrawn, licking, or shaking). All behavioral testing on animals was performed in a blinded manner.

#### 2.2.5. Measurement of paw edema

The thickness of the CFA treated paws were measured both before and after injections at the time points indicated above, using a digital caliper (Traceable Calipers, Friendswood, TX). Data were recorded to the

JPET#249904

nearest  $\pm 0.01$  mm and expressed as change in paw thickness ( $\Delta PD$  = difference in the ipsilateral paw diameter before and after injection).

#### 2.2.6. Locomotor Activity and motor coordination measures

We measured the impact of *p*-CF<sub>3</sub> diEPP on mouse locomotor activity and coordination in two different tests. For the locomotor activity, mice were placed into individual Omnitech (Columbus, OH) photocell activity cages (28 x 16.5 cm). Interruptions of the photocell beams (two banks of eight cells each) were recorded for the next 30 min after injection of vehicle and *p*-CF<sub>3</sub> diEPP (10 mg/kg, i.p.). Data were expressed as the number of photocell interruptions.

In a separate cohort of mice, we measured the impact of *p*-CF<sub>3</sub> diEPP on motor coordination. For that, we used the rotarod test (IITC Inc. Life Science, Woodland Hills, CA). Mice were placed on textured drums (1¼ inch diameter) to avoid slipping. When an animal fell onto the individual sensing platforms, test results were recorded. Five mice were tested at a time using a rate of 4 rpm. Naive mice were trained until they remained on the rotarod for 3 min or 180 s. Animals that failed to meet this criterion within three trials were discarded. Thirty min after the i.p. injection of vehicle or *p*-CF<sub>3</sub> diEPP (10 mg/kg, i.p.), mice were placed on the rotarod for 3 min. If a mouse fell from the rotarod during this time period, it was scored as motor impaired. Percent impairment was calculated as follows: % impairment = (180 - test time) / (180 \* 100).

#### 2.2.7. Statistical Analysis

The data were analyzed using GraphPad software, version 6.0 (GraphPad Software, Inc., La Jolla, CA) and expressed as the mean  $\pm$  S.E.M. Statistical analysis was done using the 1-way or 2-way analysis of variance test (ANOVA), followed by the post hoc Tukey's test. Unpaired student t test was used for spontaneous activity. The P values  $< 0.05$  were considered significant.

JPET#249904

### 3. RESULTS

#### 3.1. *In vitro* results

##### 3.1.1. $\alpha 7$ nAChR

In previous experiments, *p*-CF<sub>3</sub> diEPP was tested for its agonism at 30  $\mu$ M on the  $\alpha 7$  nAChR (Quadri et al., 2016). While it produced virtually no activation when applied alone, it generated large responses when co-applied with the type II PAM PNU-120596. We followed up those observations using the alternative type II PAM TQS. TQS has previously been reported to be a type II PAM (Grønlien et al. 2007) that produces no response when applied alone (data not shown). Multi-cell averaged responses showing the activation of  $\alpha 7$  nAChRs induced by *p*-CF<sub>3</sub> diEPP applied alone or co-applied with TQS are shown in **Figure 2**. Note we use net charge as the primary measurement of  $\alpha 7$  receptor function since concentration-dependent desensitization prevents the measurement of peak currents at high agonist concentrations (Papke and Papke, 2002). To better evaluate its partial agonism activity at the  $\alpha 7$  receptor, *p*-CF<sub>3</sub> diEPP was tested at a broader range of concentrations (3, 10, 30, 100, and 300  $\mu$ M) and showed virtually no activation of the  $\alpha 7$  receptor subtype when applied alone. The concentration-response curve (CRC) analysis evidenced an  $I_{\max}$  (maximum current response of agonist) of 5% (absolute value  $0.05 \pm 0.002$ ) of the 60  $\mu$ M ACh response (or 4% of ACh maximum response), with an  $EC_{50}$  (half maximal effective concentration) of  $26 \pm 2.4$   $\mu$ M (**Figure 3**, panel A).

We then focused on investigating the desensitizing effects of *p*-CF<sub>3</sub> diEPP on  $\alpha 7$  according to the reported protocol (Chojnacka et al., 2013) and at a range of concentrations larger than previously reported (Quadri et al., 2016). Though both TQS and PNU-120596 are good type II PAMs, for the present study we chose TQS over PNU-120596 since we found the latter to suffer from greater experimental variability and less consistent results compared to TQS co-applied with *p*-CF<sub>3</sub> diEPP. At the normal holding potential of -60 mV, the potentiated responses evoked by *p*-CF<sub>3</sub> diEPP (3, 10, 30, 100, and 300  $\mu$ M) co-applied with 10  $\mu$ M TQS displayed an inverted-U shape curve with a maximum at 30  $\mu$ M, corresponding to a response 13-fold greater than that induced by the 60  $\mu$ M ACh control (net charge absolute value  $12.9 \pm 4.99$  relative to 60  $\mu$ M ACh

JPET#249904

control response, **Figure 3**, panel B). These data confirmed the ability of the weak partial agonist *p*-CF<sub>3</sub> diEPP to promote and stabilize  $\alpha 7$  receptor desensitization. PAM-potentiated responses characterized by an inverted-U shape have been previously reported (Papke et al., 2015); we therefore wanted to investigate the phenomenon as related to the *p*-CF<sub>3</sub> diEPP responses. Specifically, we hypothesized that voltage-dependent channel block of  $\alpha 7$  induced by *p*-CF<sub>3</sub> diEPP may have been involved in the inverted-U shape of *p*-CF<sub>3</sub> diEPP TQS-potentiated responses. Voltage-dependent channel block has been previously reported to affect other positively charged small molecules responses (Papke et al., 2014b). To test this hypothesis, *p*-CF<sub>3</sub> diEPP was co-applied with TQS at the positive holding potential of +50 mV and the responses compared to those observed at the normal holding potential of -60 mV, according to a protocol previously used to determine channel-blocking activity (Papke et al., 2014b) (**Figure 3**, panel B). Note that while under normal conditions ACh-evoked  $\alpha 7$  responses show strong inward rectification that would preclude conducting experiments at positive potentials, this rectification is relieved with the effect of a type II PAM (Peng et al., 2013). We tested *p*-CF<sub>3</sub> diEPP at 30, 100, and 300  $\mu$ M co-applied with 10  $\mu$ M TQS to assess whether or not at +50 mV the PAM-potentiated responses would still invert at the higher concentrations of the drug. When co-applied with 10  $\mu$ M TQS on  $\alpha 7$  receptors at +50 mV, *p*-CF<sub>3</sub> diEPP displayed comparable potentiated inward currents at the three different concentrations tested (net charge absolute values of  $43.5 \pm 8.87$ ,  $42.7 \pm 5.78$ , and  $44.1 \pm 6.87$  at 30, 100, and 300  $\mu$ M, respectively) and did not display the invert-U phenomenon. According to the results, voltage-dependent channel block induced by co-application of *p*-CF<sub>3</sub> diEPP appears to be a limiting factor in the PAM-potentiated responses at the control negative holding potential.

In the absence of the PAM,  $\alpha 7$  silent agonists and very weak partial agonists are considered functional antagonists of the receptor and the drug potency can be evaluated in inhibition experiments. To investigate *p*-CF<sub>3</sub> diEPP antagonism on the  $\alpha 7$  receptor, 60  $\mu$ M ACh was co-applied with increasing concentrations of the *p*-CF<sub>3</sub> target compound (0.3, 1, 3, 10, 30, 100, and 300  $\mu$ M). The corresponding inhibition CRC evidenced an IC<sub>50</sub> (half maximal inhibitory concentration) of  $17 \pm 2$   $\mu$ M, with almost complete receptor inhibition at the highest concentration tested (only 10% of the initial control ACh responses left) (**Figure 4**, panel A). We then

JPET#249904

investigated whether the observed  $\alpha 7$  antagonism was competitive or not. To this end, 30  $\mu\text{M}$ , *p*-CF<sub>3</sub> diEPP was co-applied with increasing concentrations of ACh (0.3, 1, 3, 10, 30, 100, and 300  $\mu\text{M}$ , and 1 and 3 mM) (**Figure 4**, panel B). Compared to ACh applied alone, *p*-CF<sub>3</sub> diEPP co-application mostly affected ACh efficacy, with a 26% reduction in  $I_{\text{max}}$  ( $I_{\text{max}} = 98 \pm 4\%$  and  $73 \pm 3\%$ , respectively, relative to 60  $\mu\text{M}$  ACh control responses) while slightly affecting its potency, with a relatively small rightward shift of the  $\text{EC}_{50}$  ( $\text{EC}_{50} = 31 \pm 5\ \mu\text{M}$  and  $67 \pm 12\ \mu\text{M}$ , respectively). These results suggested both a noncompetitive and competitive antagonism of ACh responses by *p*-CF<sub>3</sub> diEPP at the  $\alpha 7$  nAChR.

Considering the ACh response inhibition and the evidence that emerged for the inverted-U shape PAM-potentiated responses of the *p*-CF<sub>3</sub> derivative, we hypothesized that  $\alpha 7$  voltage-dependent channel block by *p*-CF<sub>3</sub> diEPP was responsible for the reduced efficacy of ACh in the presence of *p*-CF<sub>3</sub> diEPP. We therefore co-applied *p*-CF<sub>3</sub> diEPP with ACh at different holding potentials (-90 mV, -70 mV, -50 mV, and -30 mV) and compared the evoked responses to respective controls obtained at the same holding potentials, to evaluate channel-blocking activity (Papke et al., 2014b) (**Figure 5**). As noted above, data at positive holding potentials were not suitable for analysis due to inward rectification of  $\alpha 7$  currents in the absence of a PAM.

As a test concentration, we used 30  $\mu\text{M}$  *p*-CF<sub>3</sub> diEPP co-applied with 60  $\mu\text{M}$  ACh, the same concentration used in the competition CRC test. The results at the different holding potentials suggest *p*-CF<sub>3</sub> diEPP voltage-dependent channel block to be a factor limiting the ACh currents, consistent with the results obtained with the PAM-potentiated currents (**Figure 3**). In the presence of *p*-CF<sub>3</sub> diEPP,  $\alpha 7$  residual ACh activation measured as net charge was  $19 \pm 5\%$  at -90 mV,  $34 \pm 7\%$  at -70 mV,  $44 \pm 5\%$  at -50 mV, and  $59 \pm 5\%$  at -30 mV. Results at the lowest (-90 mV) versus the highest two (-50 and -30 mV) holding potentials tested are statistically different, as well as data at -70 mV compared to -30 mV. These results collected at different holding potentials are therefore consistent with voltage-dependent channel block limiting the ACh responses that were co-applied with the *p*-CF<sub>3</sub> compound, and possibly the efficacy of the drug when applied alone to  $\alpha 7$  nAChR is impacted by channel block.

JPET#249904

Based on the results collected on the  $\alpha 7$  nAChR, we propose some hypothetical models representing the different conformational states distribution depending on receptor binding to the very weak partial agonist of interest  $p$ -CF<sub>3</sub> diEPP, in the presence or absence of ACh and/or TQS (**Figure 6**). These models are based on those proposed for other silent agonists (Papke et al., 2014b), which include high energy barriers for entering the open state in the absence of the PAM, rapid activation and frequent reopenings in the presence of the PAM and  $p$ -CF<sub>3</sub> diEPP, as well as concentration- and voltage-dependent block (B) as additional limiting factors.

### 3.1.2. Heteromeric nAChRs $\alpha 4\beta 2$ and $\alpha 3\beta 4$

Nicotinic receptor subtype selectivity for activation and inhibition was investigated by testing the effects of  $p$ -CF<sub>3</sub> diEPP on the heteromeric nAChRs  $\alpha 4\beta 2$  and  $\alpha 3\beta 4$  expressed in *Xenopus laevis* oocytes. When applied alone at 30  $\mu$ M to cells-expressing  $\alpha 4\beta 2$  or  $\alpha 3\beta 4$  nAChR,  $p$ -CF<sub>3</sub> diEPP did not evoke responses above our reliable limit of detection, equal to  $\approx 1\%$  our ACh controls (data not shown). To assess its antagonism,  $p$ -CF<sub>3</sub> diEPP was tested at different concentrations (0.3, 1, 3, 10, 30, 100, and 300  $\mu$ M) co-applied with ACh on  $\alpha 4\beta 2$  and  $\alpha 3\beta 4$  receptors (**Figure 7** panels A and B, respectively). On both receptor subtypes,  $p$ -CF<sub>3</sub> diEPP produced inhibition of the ACh responses, with IC<sub>50</sub> values of  $48 \pm 12 \mu$ M and  $8.3 \pm 1.5 \mu$ M on  $\alpha 4\beta 2$  and  $\alpha 3\beta 4$ , respectively. Multi-cell averages of the raw data showing inhibition of ACh-evoked responses by co-application with 30  $\mu$ M  $p$ -CF<sub>3</sub> diEPP at the heteromeric receptors  $\alpha 4\beta 2$  and  $\alpha 3\beta 4$  and at the homomeric  $\alpha 7$  subtype are shown in **Figure 8**. It is interesting to note from the scaled overlays at the bottom of **Figure 8** that only the  $p$ -CF<sub>3</sub> diEPP-inhibited currents of  $\alpha 7$  appear to have accelerated kinetics, often indicative of open channel block (Francis and Papke, 1996; Papke et al., 1994), suggesting that inhibition of heteromeric receptors may be mechanistically different.

### 3.2. In vivo results



JPET#249904

### 3.2.1. *p*-CF<sub>3</sub> diEPP dose-dependently attenuates CFA-induced inflammatory pain in an $\alpha$ 7-nAChR-dependent manner.

The tested compound *p*-CF<sub>3</sub> diEPP dose-dependently reduced CFA-induced mechanical hypersensitivity ( $F_{\text{dose} \times \text{time}(15,144)} = 8.41, P < 0.0001$ ; **Figure 9**, panel A). While being effective also at lower dosages of 1 and 3.3 mg/kg, post hoc analysis revealed that 10 mg/kg *p*-CF<sub>3</sub> diEPP yielded maximal reversal of hypersensitivity similar to pretreatment baseline values at 15 to 30 min after injection. The effects of 10 mg/kg *p*-CF<sub>3</sub> diEPP decreased to half of the maximum at 1 hour after injection and became negligible at 2 hours. However, *p*-CF<sub>3</sub> diEPP at 10 mg/kg did not alter von Frey responses in sham-treated mice ( $F_{\text{dose}(5,72)} = 0.744, P > 0.05$  **Figure 9**, panel B), as *p*-CF<sub>3</sub> diEPP at the tested dose and vehicle provided comparable responses.

We next evaluated the possible role of  $\alpha$ 7 nAChRs in the antinociceptive and anti-edema effects of *p*-CF<sub>3</sub> diEPP in the CFA model and sought to confirm that the effects of *p*-CF<sub>3</sub> diEPP were mediated by the  $\alpha$ 7 receptor subtype. To this end, we tested the effects of methyllycaconitine (MLA) on *p*-CF<sub>3</sub> diEPP anti-inflammatory effects in two different experiments. Systemic (10 mg/kg) administration of the  $\alpha$ 7 nAChR antagonist MLA prevented the anti-allodynic effects of *p*-CF<sub>3</sub> diEPP (10 mg/kg, i.p.) ( $F(6,24) = 66.44, P < 0.0001$ ; **Figure 10**, panel A). Indeed, administration of *p*-CF<sub>3</sub> diEPP after MLA pretreatment resulted in suppression of *p*-CF<sub>3</sub> diEPP anti-inflammatory effects by giving responses comparable to the control vehicle treated mice. Similarly, MLA (10 mg/kg; s.c.) totally blocked the anti-edema effect of 10 mg/kg *p*-CF<sub>3</sub> diEPP ( $F(6,18) = 16.01, P < 0.0003$ ; **Figure 10**, panel B). Administration of 10mg/kg i.p of *p*-CF<sub>3</sub> diEPP significantly reduced the paw edema induced by CFA injection, and this effect was completely prevented when MLA was administered prior to *p*-CF<sub>3</sub> diEPP.

### 3.2.2. *p*-CF<sub>3</sub> diEPP does not alter motor activity or motor coordination

To establish that the observed effects of *p*-CF<sub>3</sub> diEPP in the CFA-induced mechanical hypersensitivity were not due to interference in locomotor activity and coordination during the experiments, we evaluated the effects of *p*-CF<sub>3</sub> diEPP on mice locomotor activity and motor coordination at the highest effective dose in the

JPET#249904

antinociceptive tests. As seen in **Figure 11**, 10 mg/kg (i.p.) *p*-CF<sub>3</sub> diEPP, a dose that totally reversed mechanical hypersensitivity, did not affect spontaneous locomotor activity ( $t = 0.02446$ ,  $df = 14$ ;  $P > 0.05$ ) or performance in the rotarod test ( $t = 0.3132$ ,  $df = 14$ ;  $P > 0.05$ ). Although these are not direct indicators of autonomic function, which might be compromised by ganglionic ( $\alpha 3\beta 4$  nAChR) blockade, they are consistent with animals that are not behaviorally impaired by autonomic dysfunction.

#### 4. DISCUSSION

$\alpha 7$  nAChR involvement in the regulation of inflammatory processes has drawn interest for targeting this receptor subtype for treatment of inflammation and pain-related diseases (de Jonge and Ulloa, 2007; Medhurst et al., 2008; Munro et al., 2012). In the present study we investigated the *in vitro* and *in vivo* properties of *p*-CF<sub>3</sub> diEPP, a very weak partial agonist that strongly desensitizes rather than activates  $\alpha 7$  nAChR. Following up preliminary *in vitro* data on *p*-CF<sub>3</sub> diEPP, we characterized *p*-CF<sub>3</sub> diEPP over a full concentration-response range and confirmed that even at high concentrations it showed only very weak partial agonism ( $I_{\max}$  4% of ACh maximum).

To reveal the PAM-sensitive desensitized state of the  $\alpha 7$  receptor induced by *p*-CF<sub>3</sub> diEPP, we co-applied it with the type II PAM, TQS. Type II PAMs act on an  $\alpha 7$  desensitized state by destabilizing it and inducing its kinetically coupled PAM-dependent conductive state (Williams et al., 2011a). This destabilization prompts prolonged receptor activation, which can be measured in two electrode voltage-clamp experiments, and highlights the ability of some weak partial agonists that we characterize as silent agonists, to induce high levels of PAM-sensitive  $\alpha 7$  receptor desensitization. Our preliminary results on the PAM-potentiated net charge currents showed 30  $\mu$ M *p*-CF<sub>3</sub> diEPP co-application with PNU-120596 to evoke a response 62-fold greater than the one evoked by the 60  $\mu$ M ACh control, indicating the induction of the D<sub>s</sub> state by *p*-CF<sub>3</sub> diEPP (Quadri et al., 2016). We further investigated the desensitizing effects of *p*-CF<sub>3</sub> diEPP on  $\alpha 7$  by co-application with the alternative type II PAM TQS and at a broader range of concentrations. As noted above, for the present studies

JPET#249904

TQS was selected over PNU-120596 given our empirical observation of lower experimental variability and higher reproducibility when co-applied with *p*-CF<sub>3</sub> diEPP.

Similar to previous findings with the silent agonist NS6740 (Papke et al., 2015), the PAM-potentiated CRC of *p*-CF<sub>3</sub> diEPP showed an inverted-U shape. Investigation of *p*-CF<sub>3</sub> diEPP effects on ACh activation confirmed that it was a functional antagonist, consistent with the co-application of a weak partial agonist with a full agonist. However, competition experiments suggested that the compound additionally acted as a noncompetitive antagonist of the  $\alpha 7$  receptor, capable of reducing ACh efficacy while also decreasing its potency. Further investigating the nature of this noncompetitive component, we determined that the inhibition was voltage-dependent, suggesting that similar noncompetitive activity might also limit the PAM-potentiated currents measured at the normal holding potential. The competition and voltage-dependence experiments were conducted with *p*-CF<sub>3</sub> diEPP at 30  $\mu$ M, the concentration associated with the peak of the inverted-U in the TQS-potentiated responses, and presumably concentrations greater than 30  $\mu$ M of *p*-CF<sub>3</sub> diEPP would show progressively higher degrees of  $\alpha 7$  noncompetitive antagonism, resulting in the inverted-U. We confirmed that at a holding potential of +50 mV, there was little or no voltage-dependent channel block, and the *p*-CF<sub>3</sub> diEPP PAM-potentiated responses did not show an inverted-U shape, with comparable responses at the three different concentrations tested. We typically observe that the reversal potential  $\alpha 7$  currents in oocytes is approximately -10 mV, so the driving force for outward currents at +50 mV would be only 20% greater than for inward currents at -60 mV. However, the 30  $\mu$ M potentiated outward currents at +50 mV, compared to -60 mV ACh controls, were three-fold larger than the 30  $\mu$ M potentiated outward currents at -60 mV, compared to -60 mV ACh controls. These results suggest that, even at the normal holding potential, voltage-dependent channel block induced by *p*-CF<sub>3</sub> diEPP limits both apparent efficacy as an agonist and the PAM-potentiated responses.

We further evaluated the effects of *p*-CF<sub>3</sub> diEPP on heteromeric  $\alpha 4\beta 2$  and  $\alpha 3\beta 4$  nAChR expressed in *Xenopus laevis* oocytes. The  $\alpha 4\beta 2$  subunits are a model for the primary high-affinity nicotine receptors of brain, while the  $\alpha 3\beta 4$  subunits are associated with autonomic ganglia and the adrenal gland (Papke, 2014a). While no agonist activity was detected, *p*-CF<sub>3</sub> diEPP displayed inhibition of both heteromeric receptor subtypes at

JPET#249904

potencies that were similar for  $\alpha 7$ . The mechanism of antagonism was not investigated for the heteromeric receptors, although it should be noted that it was readily reversible (not shown). Additionally, as inspection of the raw data suggested, inhibition of heteromeric receptors may be qualitatively different from the inhibition of  $\alpha 7$ , since response kinetics of the heteromeric receptors were relatively unaffected (**Figure 8**). The brain penetration of *p*-CF<sub>3</sub> diEPP is unknown, so it is unclear whether there would be *in vivo* effects associated with  $\alpha 4\beta 2$  inhibition. The closely related compound ASM024 is not considered BBB penetrant (Assayag et al., 2014). Furthermore, it seems unlikely that antagonism of either  $\alpha 3\beta 4$  or  $\alpha 4\beta 2$  would have many serious aversive effects given the historical use of the CNS-penetrant potent ganglionic antagonist mecamylamine as an antihypertensive therapy (Moyer, et al. 1955, McQueen and Smirk 1957).

Our *in vivo* data demonstrated that *p*-CF<sub>3</sub> diEPP is effective in mouse models of hyperalgesia and edema and linked its activity to  $\alpha 7$  nAChR mechanisms, based on the effects of preapplication of the  $\alpha 7$ -selective antagonist MLA. The analgesic-like properties of *p*-CF<sub>3</sub> diEPP shown by our *in vivo* data could be ascribed to  $\alpha 7$  signaling pathways independent from classical agonist ion channel activation, similarly to NS6740 (Papke et al., 2015). As mentioned above, the target compound lacked significant agonist activity and, indeed, behaves as an antagonist of  $\alpha 7$  ion channel currents. Nonetheless, it promotes desensitized states of the receptor, as revealed by potentiated responses evoked by PAM co-application. Future studies could correlate the different non-conducting states wherein the receptor can exist with the anti-inflammatory effects reported here.

Because of its permanent positive charge, *p*-CF<sub>3</sub> diEPP is most likely prevented from crossing the blood-brain barrier, and therefore its anti-inflammatory activity would be most likely localized and confined to peripheral immune cells. Such compartmentalization could possibly confer the compound of interest selectivity of action on peripheral over central systems. While standard  $\alpha 7$  nAChR agonists have shown beneficial effects in chronic pain models in some studies (Gao et al., 2010; see Bagdas et al., 2017 for review), this effect was not consistently seen in others. Interestingly, agents that have been shown to be effective *in vivo* have a remarkable range of pharmacological properties, ranging from the profoundly desensitizing agent NS6740 (Papke et al.,

JPET#249904

2015) to the potent allosteric ago-PAM GAT107 (Bagdas et al., 2016). What these agents have in common is their ability to induce non-conducting states that apparently mediate signal transduction (Papke et al., 2017). The results of this study and previous work identify multiple compounds, structurally unrelated, that have anti-inflammatory effects associated with the  $\alpha 7$  nAChR. Are there unifying principles to develop a single structure activity relationship (SAR), or are their multiple SARs that have yet to be established? The answers to these questions represent the backdrop for additional design considerations. It is a concern that certain compounds may also have undesirable side effects. For example, NS6740 has been shown to antagonize the pro-cognitive effects of other  $\alpha 7$  channel activators (Briggs et al., 2009; Pieschl et al., 2017) and may directly reduce synaptic function in the hippocampus (Papke et al., submitted). Like GAT107, the type II PAM PNU-120596 is an extremely effective PAM that has been shown to be an active regulator of the cholinergic anti-inflammatory pathway (Freitas et al., 2013a; Freitas et al., 2013b). However, extreme levels of  $\alpha 7$  channel activation by PNU-120596 have also been implicated to have cytotoxic effects due to calcium overload (Guerra-Alvarez et al., 2015; Williams et al., 2012). Due to these potential limitations, a compound like *p*-CF<sub>3</sub> diEPP may represent an ideal middle road for future therapeutic development, inducing signal-transducing states without the likelihood of reducing cognitive function or cytotoxic effects.

In conclusion, these data shed light on the therapeutic potential of *p*-CF<sub>3</sub> diEPP as well as other  $\alpha 7$  very weak partial agonists for the treatment of inflammation and hyperalgesia by selectively targeting  $\alpha 7$  nAChRs desensitized conformations.

JPET#249904

## **Acknowledgments**

The authors thank Alexander den Boef for conducting the OpusXpress experiments.

JPET#249904

## **Authorship Contributions**

Participated in research design: Quadri, Papke, Horenstein, Damaj.

Conducted experiments: Bagdas, Toma, Stokes.

Contributed new reagents or analytic tools: Quadri, Horenstein.

Performed data analysis: Quadri, Bagdas, Toma, Papke, Damaj.

Wrote or contributed to the writing of the manuscript: Quadri, Papke, Horenstein, Damaj.

JPET#249904

## REFERENCES

- Assayag EI, Beaulieu M, and Cormier Y (2014) Bronchodilatory and Anti-Inflammatory Effects of ASM-024, a Nicotinic Receptor Ligand, Developed for the Treatment of Asthma. *PLoS ONE* 9(1): e86091 doi:10.1371/journal.pone.0086091.
- Bagdas D, AlShararia SD, Freitas K, Tracya M, and Damaj MI (2015) The role of alpha5 nicotinic acetylcholine receptors in mouse models of chronic inflammatory and neuropathic pain. *Biochem Pharmacol* 97(4): 590-600.
- Bagdas D, Gurun MS, Flood P, Papke RL, and Damaj MI (2017) New Insights on Neuronal Nicotinic Acetylcholine Receptors as Targets for Pain and Inflammation: A Focus on  $\alpha 7$  nAChRs. *Curr Neuropharmacol* doi: 10.2174/1570159X15666170818102108.
- Bagdas D, Wilkerson JL, Kulkarni A, Toma W, AlSharari S, Gul Z, Lichtman AH, Papke RL, Thakur GA, and Damaj MI (2016) The alpha7 nicotinic receptor dual allosteric agonist and positive allosteric modulator GAT107 reverses nociception in mouse models of inflammatory and neuropathic pain. *Br J Pharmacol* 173: 2506-2520.
- Briggs CA, Gronlien JH, Curzon P, Timmermann DB, Ween H, Thorin-Hagene K, Kerr P, Anderson DJ, Malysz J, Dyhring T, Olsen GM, Peters D, Bunnelle WH, and Gopalakrishnan M (2009) Role of channel activation in cognitive enhancement mediated by alpha7 nicotinic acetylcholine receptors. *Br J Pharmacol* 158(6): 1486-1494.
- Chaplan SR, Bach FW, Pogrel JW, Chung JM, and Yaksh TL (1994) Quantitative assessment of tactile allodynia in the rat paw. *J Neurosci Methods* 53(1): 55-63.
- Chojnacka K, Papke, RL, and Horenstein NA (2013) Synthesis and evaluation of a conditionally-silent agonist for the  $\alpha 7$  nicotinic acetylcholine receptor. *Bioorg Med Chem Lett* 23(14): 4145-4149.
- de Jonge WJ, and Ulloa L (2007) The alpha7 nicotinic acetylcholine receptor as a pharmacological target for inflammation. *Br J Pharmacol* 151(7): 915-929.



JPET#249904

- de Jonge WJ, van der Zanden EP, The FO, Bijlsma MF, van Westerloo DJ, Bennink RJ, Berthoud HR, Uematsu S, Akira S, van den Wijngaard RM, and Boeckstaens GE (2005) Stimulation of the vagus nerve attenuates macrophage activation by activating the Jak2-STAT3 signaling pathway. *Nat Immunol* 6(8): 844-851.
- Dixon WJ (1965) The up-and-down method for small samples. *J Am Stat Assoc* 60(312): 967-978.
- Francis MM, and Papke RL (1996) Muscle-type Nicotinic Acetylcholine Receptor Delta Subunit Determines Sensitivity to Noncompetitive Inhibitors while Gamma Subunit Regulates Divalent Permeability. *Neuropharm* 35(11): 1547-1556.
- Freitas K, Carroll FI, and Damaj MI (2013a) The antinociceptive effects of nicotinic receptors alpha7-positive allosteric modulators in murine acute and tonic pain models. *J Pharmacol Exp Ther* 344: 264-275.
- Freitas K, Ghosh S, Carroll FI, Lichtman AH, and Damaj MI (2013b) Effects of alpha7 positive allosteric modulators in murine inflammatory and chronic neuropathic pain models. *Neuropharmacology* 65: 156-164.
- Fujii T, Mashimo M, Moriwaki Y, Misawa H, Ono S, Horiguchi K, and Kawashima K (2017) Expression and Function of the Cholinergic System in Immune Cells. *Front Immunol* 8: 1085.
- Gao B, Hierl M, Clarkin K, Juan T, Nguyen H, van der Valk M, Deng H, Guo W, Lehto SG, Matson D, McDermott JS, Knop J, Gaida K, Cao L, Waldon D, Albrecht BK, Boezio AA, Copeland KW, Harmange JC, Springer SK, Malmberg AB, and McDonough SI (2010) Pharmacological effects of nonselective and subtype-selective nicotinic acetylcholine receptor agonists in animal models of persistent pain. *Pain* 149(1): 33-49.
- Grønlien JH, Håkerud M, Ween H, Thorin-Hagene K, Briggs CA, Gopalakrishnan M, and Malysz J (2007) Distinct Profiles of  $\alpha 7$  nAChR Positive Allosteric Modulation Revealed by Structurally Diverse Chemotypes. *J Mol Pharmacol* 72: 715-724.
- Guerra-Alvarez M, Moreno-Ortega AJ, Navarro E, Fernandez-Morales JC, Egea J, Lopez MG, and Cano-Abad MF (2015) Positive allosteric modulation of alpha-7 nicotinic receptors promotes cell death by inducing Ca(2+) release from the endoplasmic reticulum. *J Neurochem* 133(3): 309-319.

JPET#249904

- Halevi S, Yassin L, Eshel M, Sala F, Sala S, Criado M, and Treinin M (2003) Conservation within the RIC-3 gene family. Effectors of mammalian nicotinic acetylcholine receptor expression. *J Biol Chem* 278(36): 34411-34417.
- Hartung JE, Eskew O, Wong T, Tchivileva IE, Oladosu FA, O'Buckley SC, and Nackley AG (2015) Nuclear factor-kappa B regulates pain and COMT expression in a rodent model of inflammation. *Brain Behav Immun* 50: 196-202.
- Horenstein NA, and Papke RL (2017) Anti-inflammatory Silent Agonists. *ACS Med Chem Lett* 8(10): 989-991.
- Hurst R, Hajos M, Raggenbass M, Wall T, Higdon N, Lawson J, Rutherford-Root K, Berkenpas M, Hoffmann W, Piotrowski D, Groppi V, Allaman G, Ogier R, Bertrand S, Bertrand D, and Arneric SJ (2005) A Novel Positive Allosteric Modulator of the  $\alpha 7$  Neuronal Nicotinic Acetylcholine Receptor: *In Vitro* and *In Vivo* Characterization. *Neurosci* 25: 4396-4405.
- Kabbani N, and Nichols RA (2018) Beyond the Channel: Metabotropic Signaling by Nicotinic Receptors. *Trends Pharmacol Sci* 39(4): 354-366.
- Kabbani N, Nordman JC, Corgiat BA, Veltri DP, Shehu A, Seymour VA, and Adams DJ (2013) Are nicotinic acetylcholine receptors coupled to G proteins? *Bioessays* 35: 1025-1034.
- King JR, Nordman JC, Bridge SP, Lin M-K, and Kabbani N (2015) Identification and Characterization of a G Protein-binding Cluster in  $\alpha 7$  Nicotinic Acetylcholine Receptors. *J Biol Chem* 290(33): 20060-20070.
- Kulkarni AR, and Thakur GA (2013) Microwave-assisted expeditious and efficient synthesis of cyclopentene ring-fused tetrahydroquinoline derivatives using three-component povarov reaction. *Tetrahedron Lett* 54(48): 6592-6595.
- McQueen EG, and Smirk FH (1957) Use of mecamlamine in the management of hypertension. *Br Med J* 1(5016): 422-425.
- Medhurst SJ, Hatcher JP, Hille CJ, Bingham S, Clayton NM, Billinton A, and Chessell IP (2008) Activation of the  $\alpha 7$ -Nicotinic Acetylcholine Receptor Reverses Complete Freund Adjuvant-Induced Mechanical Hyperalgesia in the Rat Via a Central Site of Action. *J Pain* 9(7): 580-587.

JPET#249904

- Moyer JH, Ford R, Dennis E, and Handley CA (1955) Laboratory and clinical observations on mecamylamine as a hypotensive agent. *Proc Soc Exp Biol Med* 90(2): 402-408
- Munro G, Hansen RR, Erichsen HK, Timmermann DB, Christensen JK, and Hansen HH (2012) The  $\alpha 7$  nicotinic ACh receptor agonist compound B and positive allosteric modulator PNU-120596 both alleviate inflammatory hyperalgesia and cytokine release in the rat. *Br J Pharmacol* 167: 421-435.
- Papke RL (2014a) Merging old and new perspectives on nicotinic acetylcholine receptors. *Biochem Pharmacol* 89(1): 1-11.
- Papke RL, Bagdas D, Kulkarni AR, Gould T, AlSharari SD, Thakur GA, and Damaj MI (2015) The analgesic-like properties of the  $\alpha 7$  nAChR silent agonist NS6740 is associated with non-conducting conformations of the receptor. *Neuropharmacology* 91:34-42.
- Papke RL, Chojnacka K, and Horenstein NA (2014b) The Minimal Pharmacophore for Silent Agonism of the  $\alpha 7$  Nicotinic Acetylcholine Receptor. *J Pharmacol Exp Ther* 350(3): 665-680.
- Papke RL, Craig AG, and Heinemann SF (1994) Inhibition of nicotinic acetylcholine receptors by BTMPS, (Tinuvin® 770), an additive to medical plastics. *J Pharmacol Exp Ther* 268: 718-726.
- Papke RL, and Porter Papke JK (2002) Comparative pharmacology of rat and human alpha7 nAChR conducted with net charge analysis. *Br J Pharmacol* 137(1): 49-61.
- Papke RL, and Stokes C (2010) Working with OpusXpress: methods for high volume oocyte experiments. *Methods* 51(1): 121-133.
- Papke RL, Stokes C, Damaj MI, Thakur GA, Manther K, Treinin M, Bagdas D, Kulkarni AR, and Horenstein NA (2017) Persistent activation of alpha7 nicotinic ACh receptors associated with stable induction of different desensitized states. *Br J Pharmacol* doi: 10.1111/bph.13851.
- Peng C, Kimbrell MR, Tian C, Pack TF, Crooks PA, Fifer EK, and Papke RL (2013) Multiple modes of alpha7 nAChR non-competitive antagonism of control agonist-evoked and allosterically enhanced currents. *Mol Pharmacol* 84(3): 459-475.

JPET#249904

- Pieschl RL, Miller R, Jones KM, Post-Munson DJ, Chen P, Newberry K, Benitex Y, Molski T, Morgan D, McDonald IM, Macor JE, Olson RE, Asaka Y, Digavalli S, Easton A, Herrington J, Westphal RS, Lodge NJ, Zaczek R, Bristow LJ, and Li YW (2017) Effects of BMS-902483, an  $\alpha 7$  nicotinic acetylcholine receptor partial agonist, on cognition and sensory gating in relation to receptor occupancy in rodents. *Eur J Pharmacol* 807: 1-11.
- Quadri M, Matera C, Silnović A, Pismataro MC, Horenstein NA, Stokes C, Papke RL, and Dallanoce C (2017b) Identification of  $\alpha 7$  nicotinic acetylcholine receptor silent agonists based on the spirocyclic quinuclidine- $\Delta 2$ -isoxazoline scaffold: Synthesis and electrophysiological evaluation. *ChemMedChem* 12(16): 1335-1348.
- Quadri M, Papke RL, and Horenstein NA (2016) Dissection of *N,N*-diethyl-*N'*-phenylpiperazines as  $\alpha 7$  nicotinic receptor silent agonists. *Bioorg Med Chem* 24(2): 286-293.
- Quadri M, Stokes C, Gulsevin A, Felts ACJ, Abboud KA, Papke RL, and Horenstein NA (2017a) Sulfonium as a Surrogate for Ammonium: A New  $\alpha 7$  Nicotinic Acetylcholine Receptor Partial Agonist with Desensitizing Activity. *J Med Chem* 60(18): 7928-7934.
- Thomsen MS, and Mikkelsen JD (2012) The  $\alpha 7$  nicotinic acetylcholine receptor ligands methyllycaconitine, NS6740 and GTS-21 reduce lipopolysaccharide-induced TNF- $\alpha$  release from microglia. *J Neuroimmunol* 251(1-2): 65-72.
- Tracey KJ (2007) Physiology and immunology of the cholinergic antiinflammatory pathway. *J Clin Invest* 117(2): 289-296.
- Williams DK, Peng C, Kimbrell MR, and Papke RL (2012) The Intrinsically Low Open Probability of  $\alpha 7$  nAChR Can be Overcome by Positive Allosteric Modulation and Serum Factors Leading to the Generation of Excitotoxic Currents at Physiological Temperatures. *Mol Pharmacol* 82(4): 746-759.
- Williams DK, Wang J, and Papke RL (2011a) Positive allosteric modulators as an approach to nicotinic acetylcholine receptor-targeted therapeutics: advantages and limitations. *Biochem Pharmacol* 82(8): 915-930.

JPET#249904

Williams DK, Wang J, and Papke RL (2011b) Investigation of the Molecular Mechanism of the  $\alpha 7$  Nicotinic Acetylcholine Receptor Positive Allosteric Modulator PNU-120596 Provides Evidence for Two Distinct Desensitized States. *Mol Pharmacol* 80(6): 1013-1032.

Zdanowski R, Krzyżowska M, Ujazdowska D, Lewicka A, and Lewicki S (2015) Role of  $\alpha 7$  nicotinic receptor in the immune system and intracellular signaling pathways. *Cent Eur J Immunol* 40(3): 373-379.

JPET#249904

## Footnotes

This research was supported by the National Institutes of Health National Institute of General Medical Sciences [Grant R01-GM57481] and a fellowship from the University of Milan to MQ.

JPET#249904

## Figure legends

**Figure 1.** *Selected  $\alpha 7$  nAChR ligand structures.*

**Figure 2.** *Multi-cell averaged data traces for  $\alpha 7$  responses induced by application of  $p$ -CF<sub>3</sub> diEPP alone or co-applied with TQS. Averaged normalized responses to  $p$ -CF<sub>3</sub> diEPP compared and scaled to ACh controls. The upper traces are the averaged responses of cells to 60  $\mu$ M ACh ( $n = 5$ ) obtained prior to the application of 30  $\mu$ M  $p$ -CF<sub>3</sub> diEPP. The average ACh control peak current amplitude was  $5.05 \pm 0.65 \mu$ A, as represented by the scale bar. The lower traces are the averaged responses of cells to 60  $\mu$ M ACh ( $n = 8$ ) compared to the averaged response to the co-application of 30  $\mu$ M  $p$ -CF<sub>3</sub> diEPP and 10  $\mu$ M TQS. The average ACh control peak current amplitude was  $3.68 \pm 0.76 \mu$ A, as represented by the scale bar. Each trace of 10,322 points is 206.44 s long. Responses of individual cells were each normalized to their responses to 60  $\mu$ M ACh prior to the experimental applications. Shown are the averaged normalized responses (solid lines)  $\pm$  SEM (tan area).*

**Figure 3.** *Concentration-response curve (CRC) data for the  $\alpha 7$  nAChR responses evoked by  $p$ -CF<sub>3</sub> diEPP applied alone or co-applied with TQS. (A)  $\alpha 7$  orthosteric activation evoked by  $p$ -CF<sub>3</sub> diEPP applied alone at 3, 10, 30, 100, and 300  $\mu$ M measured as net charge. Each point is the average ( $\pm$  SEM) of at least five cells, normalized to 60  $\mu$ M ACh control responses from the same cells. (B)  $\alpha 7$  activation evoked by  $p$ -CF<sub>3</sub> diEPP (3, 10, 30, 100, and 300  $\mu$ M) co-applied with 10  $\mu$ M TQS at -60 mV (red, left side scale) and at +50 mV (blue, right side scale). The responses are reported as net charge and normalized to the average net charge value of two control applications of ACh (60  $\mu$ M) at -60 mV. Each data point represents the average normalized response of at least four cells ( $\pm$  S.E.M.).*

**Figure 4.** *Concentration-response curve (CRC) data for the  $\alpha 7$  nAChR antagonism induced by  $p$ -CF<sub>3</sub> diEPP. The responses are reported as net charge and normalized to the average net charge value of two control*

JPET#249904

applications of ACh (60  $\mu$ M). **(A)** Inhibition CRC for *p*-CF<sub>3</sub> diEPP at 0.3, 1, 3, 10, 30, 100, and 300  $\mu$ M co-applied with 60  $\mu$ M ACh. Each data point represents the average normalized response of at least four cells ( $\pm$  S.E.M.). **(B)** Competition CRC data (blue) for 30  $\mu$ M *p*-CF<sub>3</sub> diEPP co-applied with different ACh concentrations (0.3, 1, 3, 10, 30, 100, and 300  $\mu$ M, and 1 and 3 mM). For comparison, ACh CRC data alone (red) are shown at the same concentrations.

**Figure 5.** *Effects of voltage-dependent channel block induced by p-CF<sub>3</sub> diEPP on ACh responses at the  $\alpha$ 7 nAChR.* Responses evoked by co-application of 30  $\mu$ M *p*-CF<sub>3</sub> diEPP with 60  $\mu$ M ACh at different holding potentials (mV). The ACh residual responses measured in presence of *p*-CF<sub>3</sub> diEPP were  $0.19 \pm 0.05$  at -90 mV ( $n = 5$ ),  $0.34 \pm 0.07$  at -70 mV ( $n = 5$ ),  $0.44 \pm 0.05$  at -50 mV ( $n = 7$ ), and  $0.59 \pm 0.05$  at -30 mV ( $n = 4$ ) relative to 60  $\mu$ M ACh control responses obtained at the same potentials. Averaged raw data traces showing the effects of holding potential on the inhibition of ACh currents in presence of *p*-CF<sub>3</sub> diEPP at -90 mV and -50 mV are shown below. The control traces were scaled to have the same amplitude, and the co-application responses are relative to the controls.

**Figure 6.** *Hypothetical models for the energy landscape of the conformational states of  $\alpha$ 7 nAChR.* The conformational changes and the corresponding hypothetical energy landscape variations for the  $\alpha$ 7 receptor as affected by the binding of the very weak partial agonist *p*-CF<sub>3</sub> diEPP with or without the effects of co-applied TQS or ACh. Based on the  $\alpha$ 7 nAChR states identified in our previous studies, two forms of  $\alpha$ 7 desensitization ( $D_s$  and  $D_i$ ), a resting closed state (C), a low-probability open state ( $O^*$ ), and a PAM-dependent open state (O') that can be coupled to the  $D_s$  state are shown here. The models refer to intermediate levels of agonist and allosteric modular binding at the orthosteric and allosteric sites, respectively. Such conditions were proven to be the most effective in promoting channel opening (Williams et al., 2011b). For each model, the vertical displacement of the states represents the absolute free energy of the various states, and the height of the energy barriers are inversely related to the rate constants for transitions between the states and are represented by the



JPET#249904

lines connecting the states. When no ligands are bound, the C state is most stable and transitions to other states are thermodynamically unlikely to happen. Once *p*-CF<sub>3</sub> diEPP is applied, the thermodynamic landscapes of  $\alpha 7$  receptors would rearrange in such a way that the probability of entering O\* is somewhat increased but still low. Transition to the D<sub>s</sub> or D<sub>i</sub> states becomes most likely. Upon application of TQS alone, the receptor is less likely to enter the desensitized state, and the additional O' state enters the energy landscapes; however, channels are still unlikely to open. When *p*-CF<sub>3</sub> diEPP is co-applied with TQS, the type II PAM favors the transition from D<sub>s</sub> to the O', resulting in prolonged bursts of receptor openings. The channel blocking components of *p*-CF<sub>3</sub> diEPP (B) affect both the low-probability open state (O\*) and a PAM-dependent open state (O').

**Figure 7.** Concentration-response studies (CRCs) for *p*-CF<sub>3</sub> diEPP at the heteromeric nAChRs  $\alpha 4\beta 2$  and  $\alpha 3\beta 4$ .

The data represent the inhibition of receptor subtypes induced by co-application of *p*-CF<sub>3</sub> diEPP (0.3, 1, 3, 10, 30, 100, and 300  $\mu$ M) with ACh control (100  $\mu$ M for  $\alpha 3\beta 4$  and 30  $\mu$ M for  $\alpha 4\beta 2$ ) at the  $\alpha 4\beta 2$  (A) and  $\alpha 3\beta 4$  (B) nAChRs. The responses are measured as peak current and normalized to ACh control applied alone. Each data point is the average normalized response of at least four cells ( $\pm$  S.E.M.).

**Figure 8.** Multi-cell averaged raw data traces for inhibition of ACh-evoked responses by co-applications with 30  $\mu$ M *p*-CF<sub>3</sub> diEPP. The top traces are the averaged responses of cells (n = 5) expressing  $\alpha 7$  nAChR to 60  $\mu$ M ACh alone or co-applied with *p*-CF<sub>3</sub> diEPP. The average ACh control peak current amplitude was  $2.46 \pm 0.38$   $\mu$ A. The middle traces are the averaged responses of cells (n = 5) expressing  $\alpha 4\beta 2$  nAChR to 30  $\mu$ M ACh alone or co-applied with *p*-CF<sub>3</sub> diEPP. The average ACh control peak current amplitude was  $3.19 \pm 0.62$   $\mu$ A. The bottom traces are the averaged responses of cells (n = 7) expressing  $\alpha 3\beta 4$  nAChR to 30  $\mu$ M ACh alone or co-applied with *p*-CF<sub>3</sub> diEPP. The average ACh control peak current amplitude was  $1.05 \pm 0.15$   $\mu$ A. Each trace of 10,322 points is 206.44 s long. Responses of individual cells were each normalized to their responses to ACh (60  $\mu$ M, 30  $\mu$ M, and 100  $\mu$ M, respectively) prior to the experimental applications. Shown are the averaged

JPET#249904

normalized responses (solid lines)  $\pm$  SEM (tan area). Shown at the bottom are kinetic comparisons of control and  $p$ -CF<sub>3</sub> diEPP inhibited currents scaled to the same amplitude.

**Figure 9.** *The effects of systemic  $p$ -CF<sub>3</sub> diEPP in the complete Freund's adjuvant (CFA)-induced chronic inflammatory pain model. (A)* Antiallodynic effects after i.p. administration of various doses of  $p$ -CF<sub>3</sub> diEPP (1, 3.3, and 10 mg/kg). The mechanical paw withdrawal thresholds were determined 3 days after i.pl. injection of CFA (50%). **(B)** The effects of  $p$ -CF<sub>3</sub> diEPP at 10 mg/kg on mechanical sensitivity after intraperitoneal injection in sham mice were determined using Von Frey test. BL: baseline; Dose 0 = Vehicle.

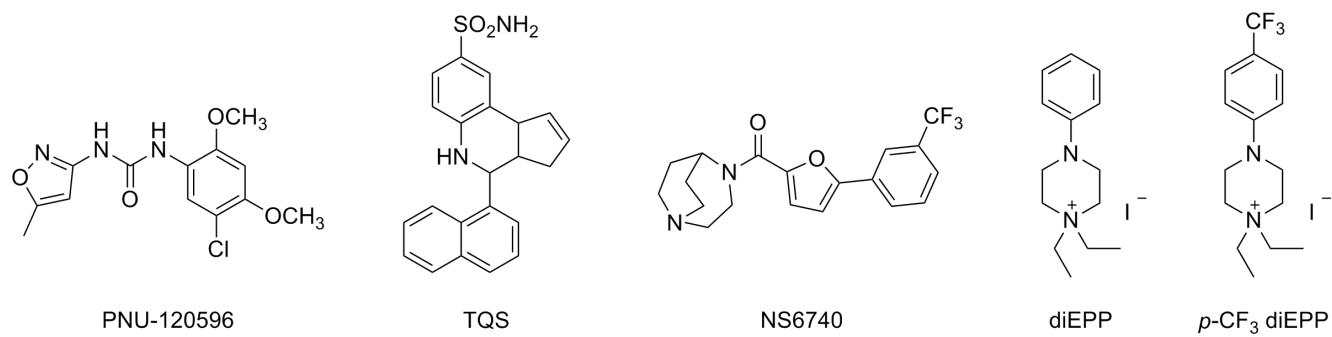
**Figure 10.** *The effects of systemic  $p$ -CF<sub>3</sub> diEPP in the complete Freund's adjuvant (CFA)-induced chronic inflammatory pain model. (A)* To determine the blockade of the antiallodynic effect of  $p$ -CF<sub>3</sub> diEPP by the  $\alpha$ 7 antagonist methyllycaconitine citrate (MLA), MLA was administered systemically (10 mg/kg, s.c.) 15 min before  $p$ -CF<sub>3</sub> diEPP (10 mg/kg, i.p.) injection and mice were tested 30 min after. \*  $P < 0.05$ , significantly different from vehicle-vehicle group; # $P < 0.05$ , significantly different from BL group. **(B)** The anti-inflammatory effect of  $p$ -CF<sub>3</sub> diEPP (10 mg/kg, i.p.) and its blockade by MLA. The effect was measured by the difference in the ipsilateral paw diameter before and after CFA injection ( $\Delta$ PD), was assessed 1 hour after  $p$ -CF<sub>3</sub> diEPP and/or MLA. Injection. \*  $P < 0.05$ , significantly different from vehicle-vehicle group. BL: baseline; Veh: Vehicle.

**Figure 11.** *Effects of  $p$ -CF<sub>3</sub> diEPP on motor activity and motor coordination in mice. (A)* Mice were placed into photocell activity cages for 30 min after 30 min i.p. administration of vehicle or  $p$ -CF<sub>3</sub> diEPP (10 mg/kg). Data are presented as mean  $\pm$  S.E.M. as the number of photocell interruptions. **(B)** Mice were placed on the rotarod for 3 min after 30 min i.p. administration of vehicle or  $p$ -CF<sub>3</sub> diEPP (10 mg/kg). Data were presented as mean  $\pm$  SEM of % impairment for each group. Data were given as the mean  $\pm$  S.E.M. of 6-8 animals for each group; Veh: Vehicle.

JPET#249904

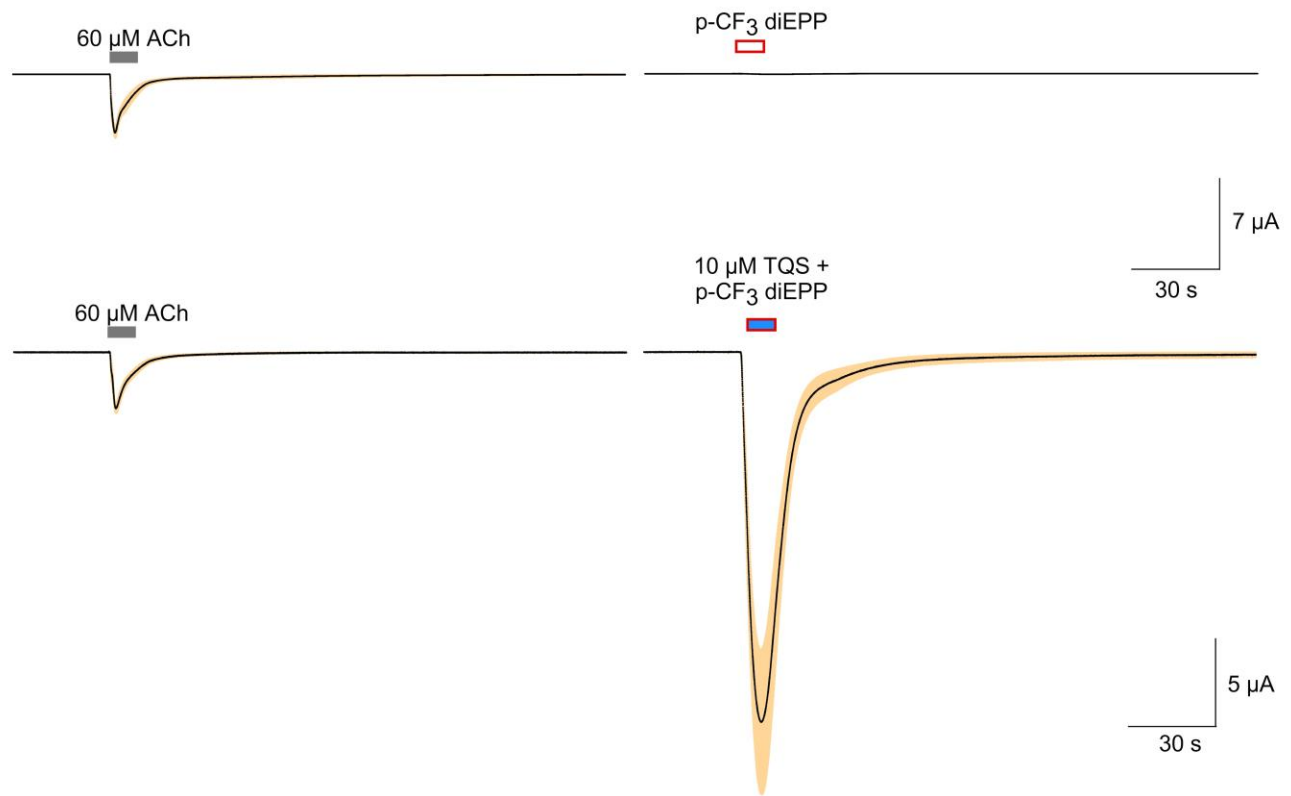
## Figures

Figure 1



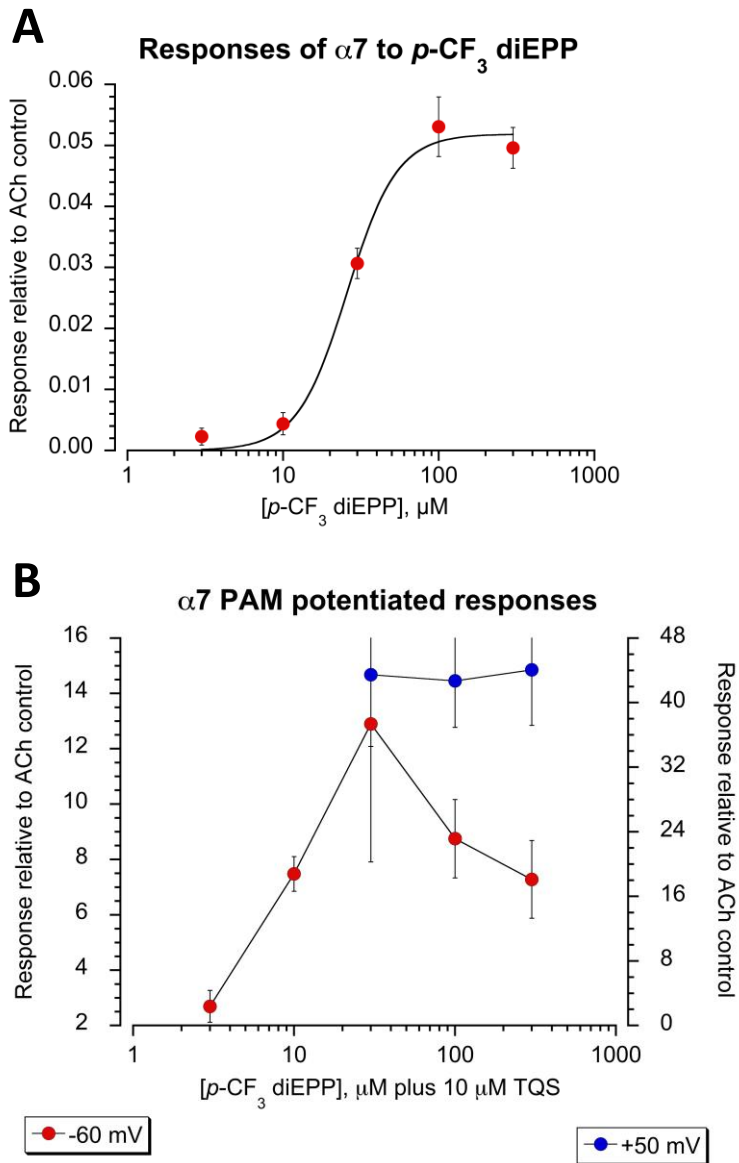
JPET#249904

**Figure 2**



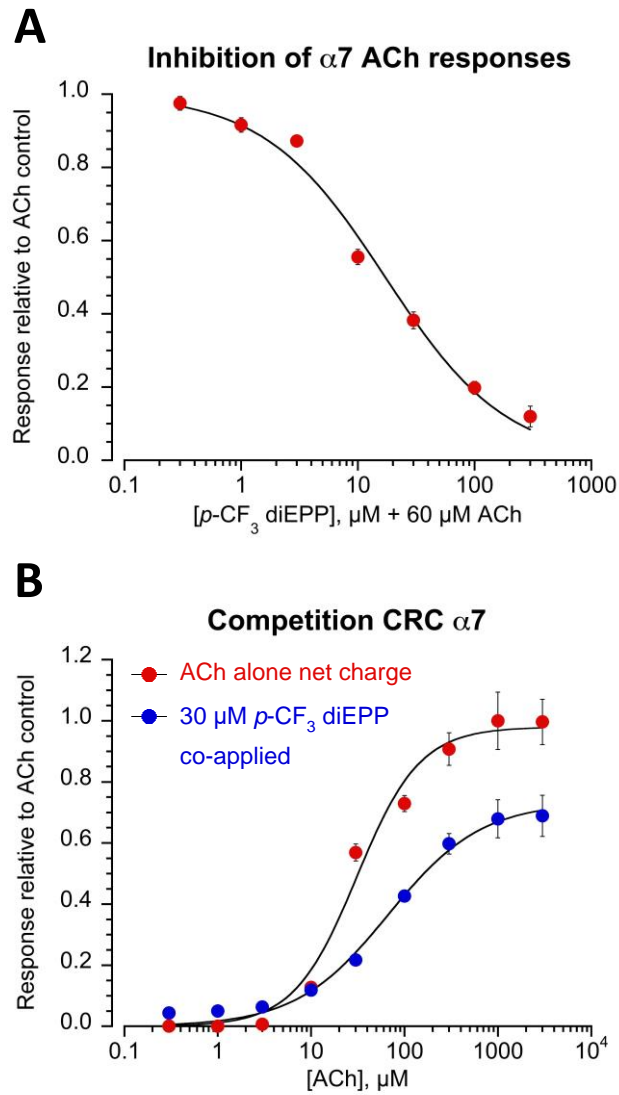
JPET#249904

Figure 3



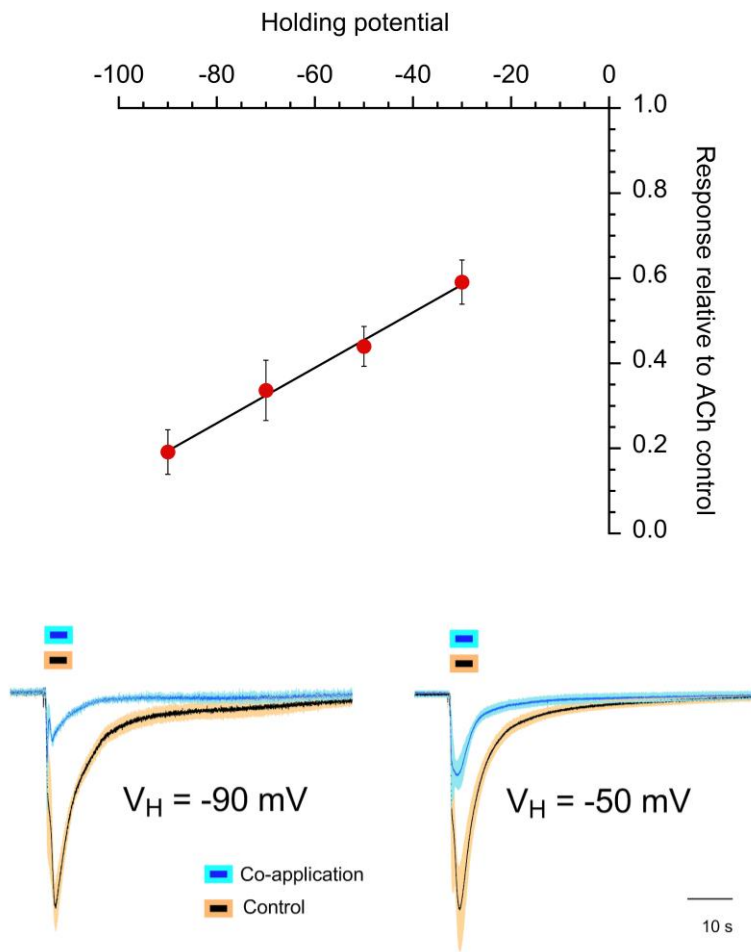
JPET#249904

Figure 4



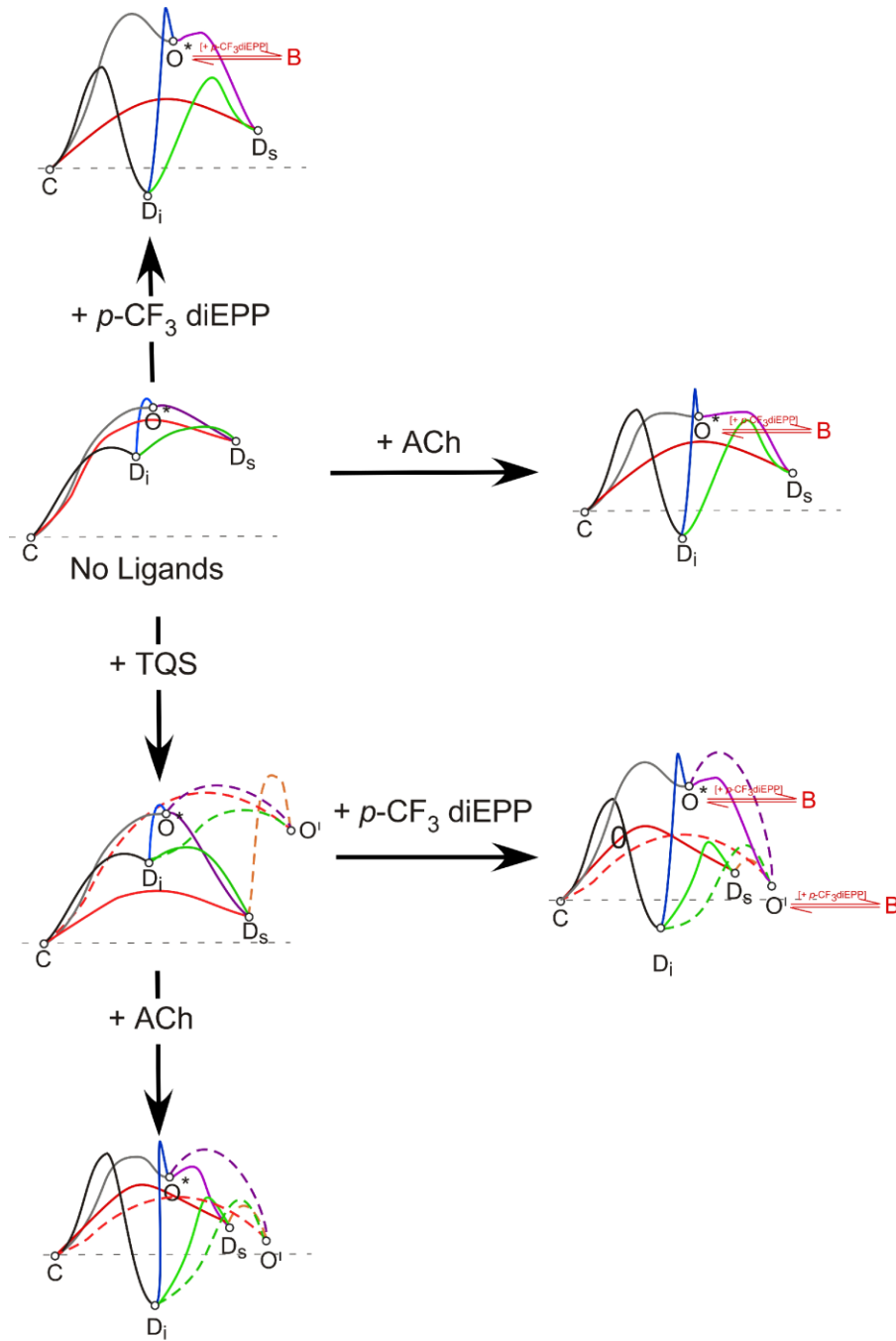
JPET#249904

Figure 5



JPET#249904

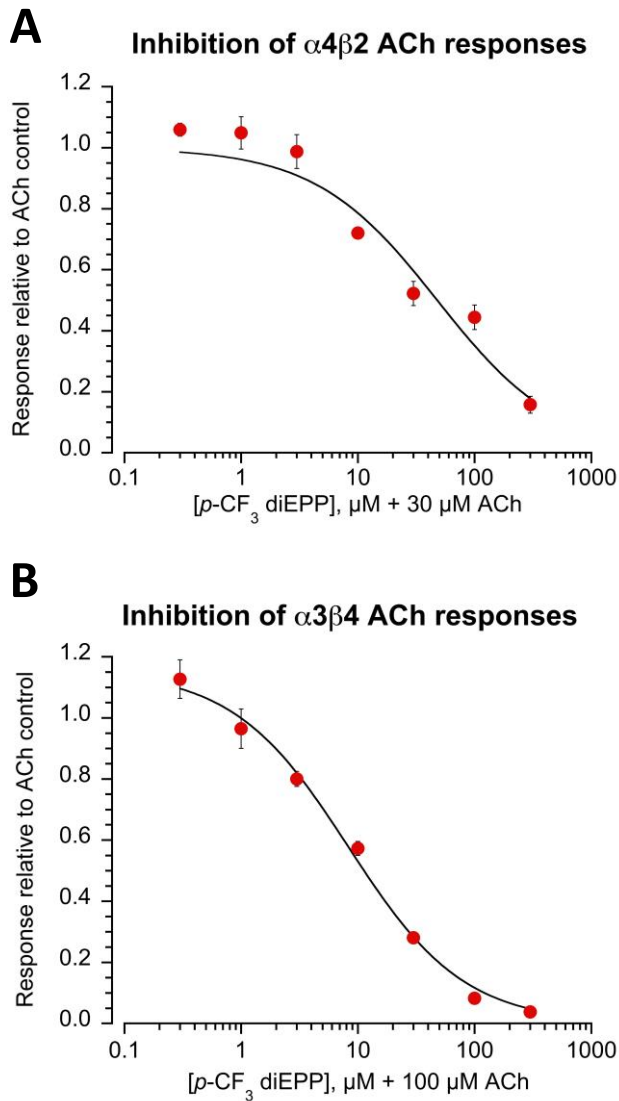
Figure 6





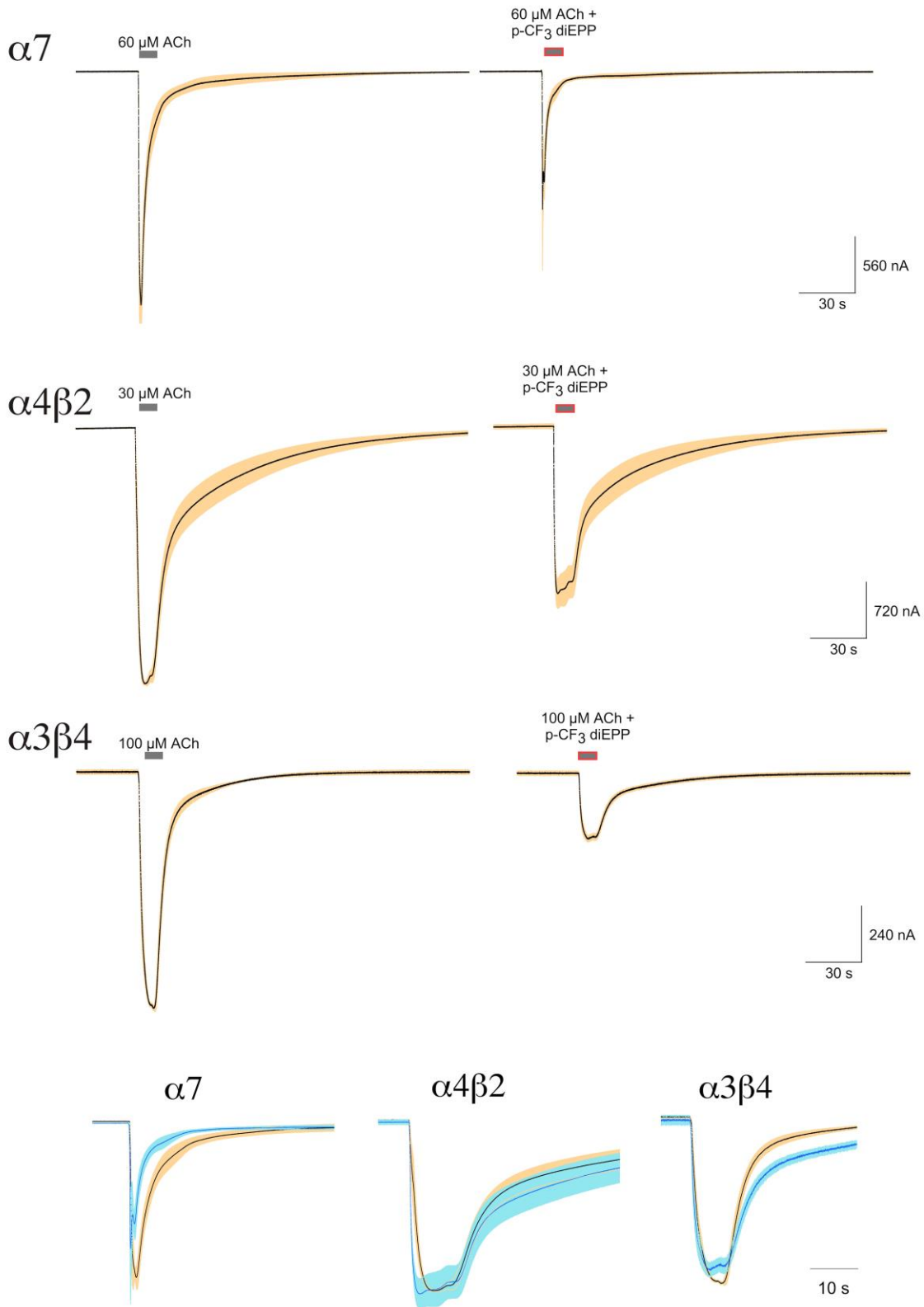
JPET#249904

Figure 7



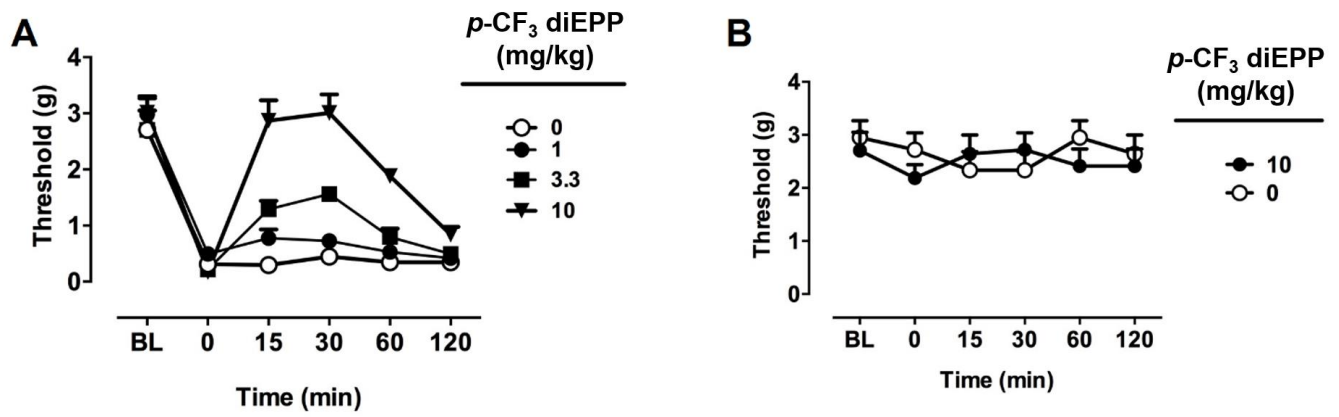
JPET#249904

Figure 8



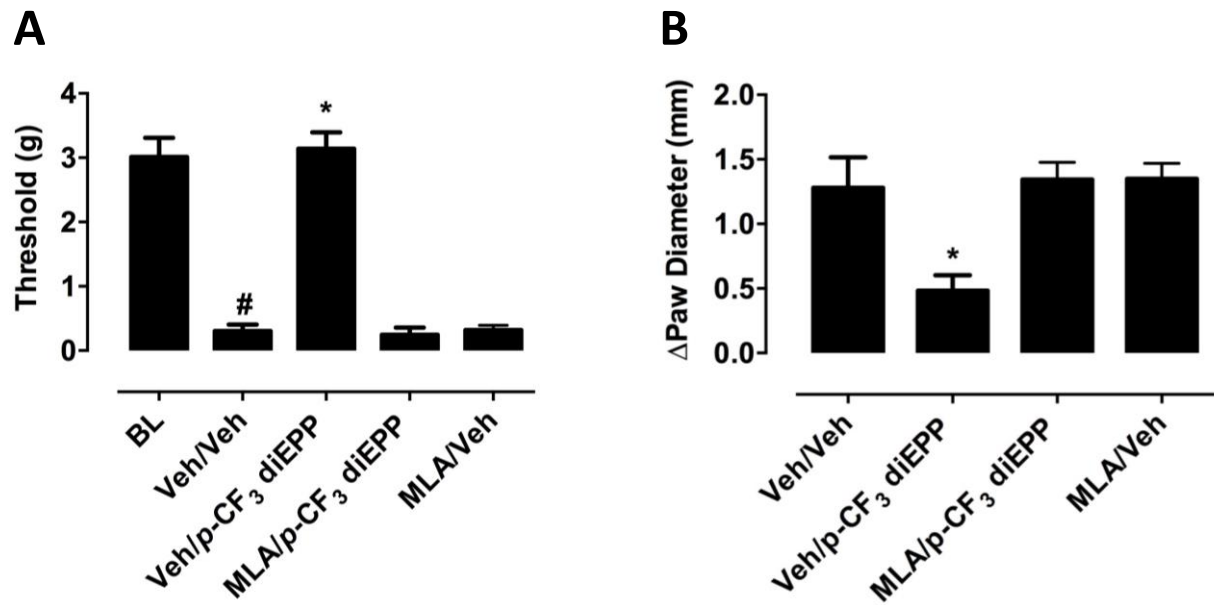
JPET#249904

Figure 9



JPET#249904

Figure 10



JPET#249904

Figure 11

